

# HIGH-BANDWIDTH AERONAUTICAL TELECOMMUNICATION OPTIONS

K.-D. BÜCHTER and A. SIZMANN

Bauhaus Luftfahrt e.V., Lyonel-Feininger-Str. 28, 80807 Munich, Germany

## Abstract

People expect being able to go online everywhere and at any time, and airlines are addressing the strong demand for mobile connectivity by equipping fleets of airliners with SATCOM antennas, which is currently the only solution for quasi-global broadband internet access. Still, bandwidth is an expensive commodity, limiting passenger acceptance. Therefore, in this paper, complementary options for broadband aeronautical communication are explored, with the prospect of unlocking additional capacities in high-capacity airborne networks. For highest bandwidth transmission through clear atmosphere, laser-links can be used, whereas RF-technologies at GHz-frequencies are required for adverse weather conditions. For highest availability, microwave frequencies are required, whereas more exotic frequencies in the millimeter-wave regime show potential for long-range stratospheric communication with limited cloud penetration capability.

## 1. INTRODUCTION

From previous analysis in [1] and [2], broadband aircraft-to-aircraft networking emerges as a promising alternative to SATCOM to overcome the bandwidth limitations thereof by transferring the aggregated capacity from single or few satellites to large and dynamic ad-hoc networks of aircraft. Due to the nature of networking and the distribution of aircraft as both data add/drop nodes and data cross-connects, the aggregated data rate which is forwarded not from one, but from several aircraft determines the bitrate capacity demand of the communication terminals. Therefore, much spectral bandwidth is needed, in turn requiring high signal carrier frequencies. The highest modulation bandwidths are achieved in fiber-optic telecommunication systems, surpassing 30 GHz per frequency channel<sup>1</sup>, and broad and unregulated spectrum is available for laser communication in atmospheric transmission windows. This means that the modulation bandwidth for *single frequency* laser links may be comparable to *the total allocated SATCOM spectrum* in Ku- and Ka-band (around 20 GHz of allocated spectrum for up- and downlink), while the available spectrum is much larger still. The modulation bandwidth typically translates to a similar bitrate capacity, assuming a spectral efficiency of the order of 1 bps/Hz. By using frequency multiplexing, i.e., DWDM (Dense Wavelength Division Multiplexing), a transmission capacity on the order of 16 Tbps can be provided for a point-to-point link in optical transmission systems. Additional techniques (e.g., polarization and modal diversity, higher order modulation formats) can enhance this potential even further [3].

In power-limited transmission scenarios, as in long distance, wireless communication, highly directive point-to-point links can offer large communication capacity, and laser communication offers the highest possible

directivity. Fiber-optic (FO) telecommunication components (e.g., semiconductor lasers, high-bandwidth photo-detectors, integrated modulators, signal regenerators and WDM components) are well-developed and much of the technology can, in principle, be transferred to free-space optical (FSO) systems, by integration with FSO terminals and the intra-plane, avionic data transport network between terminals, leveraging the performance potentials and cost efficiency in aeronautical applications.

Laser communication is a good option for ultimate bandwidth in the favorable clear-sky conditions of the stratosphere, as the atmosphere provides several optical transmission windows in the wavelength range from the visible to the infrared with low molecular absorption. However, optical signal propagation in the troposphere is often limited in range due to excessive attenuation by atmospheric aerosols and hydrosols, including especially clouds and fog, and suffers from fading due to clear-air turbulence, especially in the lower atmospheric layers.

In order to mitigate these effects for transmission in adverse weather conditions, e.g., when high altitude clouds (chiefly cirrostratus, cirrocumulus and cumulonimbus) obstruct the air-to-air, line-of-sight transmission path, as well as for resilient connectivity to the ground, we intend to investigate the future potentials of laser and radio frequency (RF) hybridization [4] for future airborne communication networks. In order to develop a better understanding of the performance potentials, a framework must be defined to compare and evaluate options for broadband aeronautical RF and laser communication. In this framework, the following considerations may play a role, depending on the respective frequency range:

- Spectrum availability (today),
- Atmospheric absorption and dispersion,
- Susceptibility to meteorological conditions (attenuation and fading by water vapor, aerosols, hydrosols, hydrometeors, turbulence),

<sup>1</sup> e.g. Covega / Thorlabs Quantum Electronics LN05S-FC LiNbO<sub>3</sub> optical phase-modulator, bandwidth: 35 GHz; bitrate: 40 Gbps.

**Table 1: Current<sup>1</sup> and possible future aeronautical connectivity options.**

Approx. frequency ranges for communication services		Allocated spectrum/approx. available channel bandwidth	Approx. cost per installed bitrate [€/kbps]
<b>Aeronautical radio-communications</b>	VHF (118-137 MHz) UHF (3-30 MHz)	19 MHz / 25 kHz 27 MHz / 25 kHz	assuming (digital) data link:  ca. 30 <sup>2</sup>
<b>Aeronautical radio-navigation</b>	VOR, ILS (108-118 MHz) ILS (330-335 MHz) DME (960-1215 MHz)	10 MHz / 50 kHz 5 MHz / 0.15 kHz 275 MHz / 0.1 kHz	
<b>Today</b>			
<b>Terrestrial (AirCell):</b>	850 MHz	4 MHz / 1.25 MHz	ca. 30-45 <sup>3</sup>
<b>SATCOM (Ku-/Ka-band):</b>	12-18, 26.5-40 GHz	20,000 MHz / 27 MHz	ca. 110 <sup>4</sup>
<b>Future possibilities</b>			
<b>AirCell:</b>	14-14.5 GHz	500 MHz / 100 MHz	assuming cost from <sup>3</sup> : ca. 1.5
<b>Microwaves:</b>	e.g., 5.6/10/30 GHz	- / 100's-1,000's MHz	N.N.
<b>Millimeter waves:</b>	e.g., 80/150/210 GHz	- / 1,000's-10,000's MHz	N.N.
<b>Optical:</b>	e.g., C-/L-band, 1.53-1.625 $\mu$ m	- / 1,000,000's MHz	ca. 0.1 <sup>5</sup>

- Interference potentials (adjacent radio systems, multipath effects, thermal radiation...) and mitigation strategies,
- Modulation formats, coding, and limitations thereof (e.g., susceptibility to Doppler shift),
- State-of-the-art technologies (antennas, beam shaping, transmitters/sources, receivers/detectors, receiver sensitivity...).

The relative impact of these considerations in the context of high-frequency stratospheric communication may differ over orders of magnitude. For example, multipath effects relevant to terrestrial cellular radio may be negligible due to separation from the ground and high directivity, whereas otherwise moderate cloud attenuation can add up to severe levels in the case of long horizontal propagation paths. The more general high-level criteria for the evaluation of telecommunication equipment are

- Capacity [bps] &
- Range [km] performance
- Reliability (fading: small scale / large scale) or Quality of Service (QoS) [% availability],
- Cost per installed bitrate [\$/bps]
- Cost per bit transmitted [\$/bit].

In this paper, an effort is made to develop a framework for the future assessment of high bandwidth transmission options for hybrid RF/photonic airborne communication networks with these criteria in mind.

## 2. SPECTRUM OVERVIEW

International spectrum allocation is managed by the ITU for frequencies between 3 kHz and 300 GHz. For aeronautical radio-communication (aeronautical mobile) and -navigation, essentially frequencies in the bands shown in Table 1 are allocated in Europe ("today"). VHF

and UHF frequency bands provide exclusive channels for communication and navigation. Arguably, frequencies currently used for radio navigation, especially for distance measuring equipment (DME), could be freed in the future for data-transmission, assuming possible obsolescence due to highly available global navigation satellite services (GNSS, e.g., GPS, GLONASS, Galileo). For broadband connectivity, *Ku*- and *Ka*-band satellite spectrum is available today as a non-exclusive resource to aviation and other customers (maritime, terrestrial). Air-to-ground connectivity is available on continental flights in certain regions, notably 4 MHz of spectrum in the 800-MHz frequency band is used by AirCell Gogo, with future plans to exploit 500 MHz of spectrum in the 14-14.5-GHz region<sup>6</sup>. At 14 GHz, attenuation by clouds and rain is moderate according to modeling presented in the following, and tolerable for air-to-ground connectivity with a dense infrastructure of ground access points.

The approximate cost for installed bitrate is shown as well. SATCOM has the highest cost per installed bitrate according to the specifications found, although the aggregated capacity is also currently the highest. Beyond the frequencies already accounted for, the millimeter-wave spectrum, as well as laser frequencies, offer future opportunity for high-altitude communications, with potential bandwidths in the GHz- or even THz-range. Due to the large bandwidth, installation cost per bitrate for laser communication is low. Installation cost for microwave or millimeter wave communication was not available at the time of writing. In order to determine total costs for economic analysis, other cost factors, such as required communication infrastructure, must also be regarded.

## 3. ATMOSPHERIC TRANSMISSION IMPAIRMENTS

The atmosphere can be described as a dynamic, layered,

<sup>2</sup> <http://www.gps.co.uk/micheltkm-mx11/p-86-162-302/>

<sup>3</sup> <http://www.duncanaviation.aero/avionics/wifi/aircell/index-b.php>

<sup>4</sup> <http://www.duncanaviation.aero/avionics/satcom/kuband.php>

<sup>5</sup> Personal communication, ViaLight Communications GmbH

<sup>6</sup> Comments of GOGO Inc., on FCC RM – 11640, 2011

inhomogeneous mixture of gas molecules, particularly oxygen, water vapor, and carbon dioxide; as well as aerosols and hydrosols, comprised of liquid water in the form of fog, clouds and precipitation, and solid particles in the form of dust and smoke of differing size distribution. All of these parameters may contribute to absorption and scattering of electromagnetic radiation with a variation in severity by orders of magnitude. Therefore, depending on transmission frequency and locations of transmitter and receiver, transmission characteristics and availability of the communication channel may vary strongly. In an aeronautical telecommunication network, long transmission range is a crucial factor due to high altitudes, high velocity, and long link spans, whereas agility is arguably less important in commercial air travel, as the network nodes are approximately at rest in a co-moving frame. Here, especially point-to-point link spans with highly directive (“high gain”) antennas can offer large communication capacity considering noise-limited transmission scenarios<sup>7</sup>. Such links typically operate in the millimeter-wave range or at infrared wavelengths (LASERCOM).

Seminal works on the modeling of millimeter-wave propagation through the atmosphere were published by Liebe (e.g., [5]), and important aspects are discussed in the remainder of this chapter. The Lambert-Beer law is used here to describe power transmittance:

$$T = \exp \left\{ - \int_0^s \alpha(s') ds' \right\} = 10^{-0.1 \int_0^s \alpha_{dB}(s') ds'}$$

considering the path variable  $s'$  and the path-dependent attenuation coefficient  $\alpha(s')$ , where  $\alpha_{dB} = 4.34 \alpha$ . For long-range communication, low attenuation is essential. The attenuation coefficient accounts for absorption and scattering mechanisms by molecules and aerosols, i.e.

$$\alpha = \alpha_{abs}^a + \alpha_{abs}^g + \alpha_{scat}^a + \alpha_{scat}^g + \dots$$

where  $a$  denotes aerosol,  $g$  denotes gas (molecules),  $abs$  denotes absorption and  $scat$  denotes scattering. Additional contributions such as non-linear scattering are not considered here due to the limited significance.

Next, the frequency dependence of dominant contributors to the attenuation coefficients is discussed.

### 3.1. Atmospheric Absorption and Scattering

Atmospheric attenuation can be substantial in the vicinity of molecular absorption lines. Moreover, aerosol may contribute to attenuation via absorption, especially in the infrared range [6]. At radio frequencies, the effect is less pronounced for non-aqueous aerosols, but it may be substantial in the case of hydrosols (water particles, such as mist, fog, or clouds).

<sup>7</sup> Multipath propagation due to scattering and reflections may be relevant or even beneficial to certain transmission schemes such as MIMO (Multiple Input – Multiple Output), in the case of non-line-of-sight communication and under otherwise interference-limited conditions.

#### 3.1.1. Molecular Absorption

Absorption due to electronic, rotational and vibrational quantum-mechanical energy transitions of molecules and combinations thereof (vibronic, rovibrational coupling) leads to a multitude of spectral absorption lines and bands affecting electromagnetic radiation, spanning from radio-frequencies all the way to the ultraviolet range at frequencies of hundreds of THz. Line-by-line databases like HITRAN [7] and GEISA [8] permit the calculation of atmospheric absorption profiles as function of wavelength and atmospheric path, depending on local parameters including temperature, pressure, and water vapor content.

Within the frequency range up to 1 THz, rotational and vibrational transitions need to be considered. The International Telecommunication Union (ITU) provides a practical model<sup>8</sup> which permits the calculation of atmospheric absorption as function of atmospheric parameters (pressure, temperature, humidity ...), using line data for H<sub>2</sub>O and oxygen absorption, and considering a semi-empirical non-resonant dry-air continuum due to pressure-induced nitrogen absorption and the Debye spectrum of oxygen.

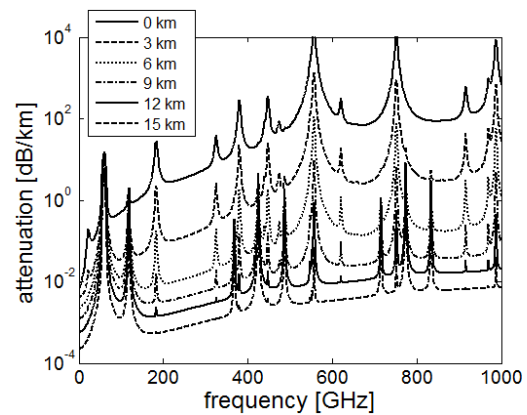


**Figure 1: Attenuation due to absorption of radio waves up to 1000 GHz as function of altitude in a standard atmosphere.**

The ITU-model was used to calculate the frequency-dependent attenuation curves in Figure 1 on the basis of modified MATLAB code published in [9] as function of altitude in a standard atmosphere [10], where a water vapor content of 7.5 g/m<sup>3</sup> was assumed at sea level with a scale height of 1 km for water vapor. Due to the large range of attenuation coefficients, attenuation in dB/km is itself depicted on a logarithmic scale, ranging from 10<sup>-4</sup> dB/km for low frequencies at high altitudes, to beyond 10<sup>4</sup> dB/km for low altitudes near absorption lines. Two trends can be observed: increasing continuum absorptivity with increasing frequency, and declining absorptivity (with less-broadened peaks) with increasing altitude, due to the thinning and cooling of air and reduced water vapor content. Near the typical cruise altitude of 10 km, attenuation is below 0.01 dB/km for frequencies lower than 400 GHz and away from

<sup>8</sup> ITU-R P676-10, “Attenuation by atmospheric gases” (09/2013)

characteristic absorption lines near 60, 120 and 180 GHz. Moreover, above 9 km, attenuation remains below 0.1 dB/km for most frequencies up to 1 THz (away from the characteristic absorption peaks). This indicates that, in principle, hitherto exotic transmission frequencies could be exploited for high-altitude, aircraft-to-aircraft (and aircraft-to-satellite) communication scenarios. Above 6 km altitude and below 400 GHz, still a number of transmission windows are found around 30, 90, 150, 210-310, and 340 GHz, with attenuation below 0.1 dB/km.

### 3.1.2. Aerosol Scattering

Rayleigh theory may be used to quantify attenuation by scattering for particle sizes smaller than the wavelength, with attenuation being proportional to the fourth power of frequency. For typical aerosol scatterers with diameters in the  $\mu\text{m}$ -range, the scattering cross-section is negligibly small, leading to also negligible attenuation in the GHz-frequency range, as can be seen in Figure 2. Scattering due to aerosols thus becomes relevant only at THz-frequencies in the case of solid particles like soot.

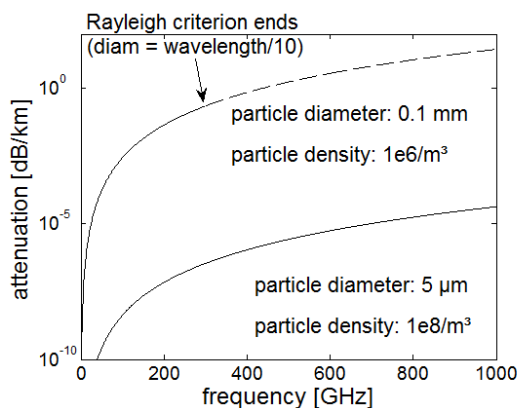


**Figure 2: Approximate attenuation due to Rayleigh-scattering, assuming fixed particle size and homogeneous particle distribution.**

At even higher frequencies in the near infrared and visible wavelength range, molecular scattering even becomes relevant. At the opposite end in the GHz-regime, only larger scatterers, especially hydrosols (cloud and fog) and hydrometeors (precipitation), need to be considered.

### 3.1.3. Cloud and Fog Attenuation

We here neglect non-aqueous aerosol absorption by solid particles and consider them to be transparent to GHz-waves, due to the notion that the effect is negligible at radio-frequency [6]. We note that solid particle aerosol absorption is relevant for infrared and visible light. Moreover, aerosol in the form of haze is chiefly limited to lower altitudes. However, hydrosols in the form of mist, fog or clouds have substantial impact on radiation at GHz-frequencies due to absorption bands in liquid water as well as scattering properties. In order to quantify the effect of fog and clouds, again the ITU recommendation<sup>9</sup> has been used to generate Figure 3.

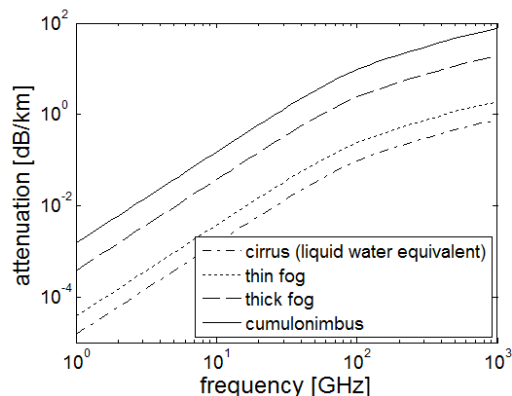


**Figure 3: Typical values of cloud and fog attenuation.**

The recommendation considers Rayleigh scattering in addition to absorption by liquid water droplets. Attenuation increases sharply with frequency and reaches 1 dB/km at 40 GHz in the case of a cumulonimbus cloud (liquid water content = 2 g/m<sup>3</sup> assumed). An attenuation of 1 dB/km can easily accumulate along horizontal paths through the atmosphere to reach unacceptable levels. Therefore, carrier frequencies beyond several 10 GHz have reduced potential for long-range communication in the troposphere, but do offer potentials for air-ground communication through cloud layers of limited extent. In the case of satellite communication, losses can be tolerated to a degree, due to the essentially vertical path through cloud layers. In the case of high-altitude cirrus clouds, attenuation is tolerable (< 0.1 dB/km) up to a frequency of about 100 GHz.

### 3.1.4. Rain scattering

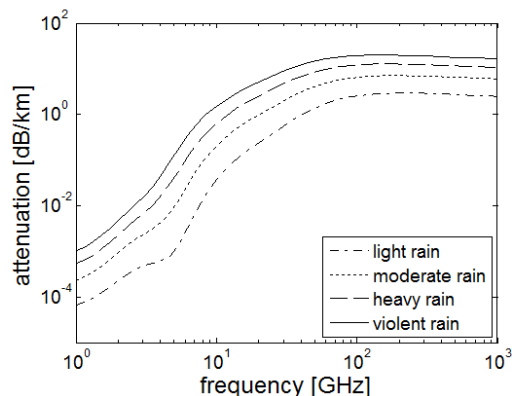


**Figure 4: Rain attenuation as function of frequency and rain severity (average of horizontal/vertical polarization states).**

For larger sized particles comparable to or larger than the wavelength, the more general Mie-scattering theory must be used to determine scattering cross-sections and attenuation. The ITU provides a model<sup>10</sup> that allows calculation of rain attenuation as function of rain rate, frequency and polarization plane, according to a power law with coefficients derived from scattering calculations.

<sup>9</sup> ITU-R P840.6, "Attenuation due to clouds and fog" (09/2013)

<sup>10</sup> ITU-R P838-3, "Specific attenuation model for rain for use in prediction methods" (03/2005)

In Figure 4, rain attenuation is given as the average of vertical and horizontal polarization components of the wave, as function of frequency and rain rate (2.5, 10, 25, and 50 mm/h rainfall assumed for light, moderate, heavy and violent rain, respectively). Apparently, attenuation becomes moderately severe (1 dB/km) in the frequency range between 8 and 40 GHz and saturates beyond 100 GHz. In the “light rain”-scenario, attenuation reaches a maximum of ca. 3 dB/km beyond 100 GHz. Already at 10 GHz, heavy rain may generate 1-dB attenuation per kilometer.

### 3.2. Temporal effects

#### 3.2.1. Group Velocity Dispersion

Group velocity dispersion (GVD) describes temporal broadening of pulses due to retardation of its frequency components, due to refractive index dispersion. GVD can be detrimental if the broadened pulse width surpasses the separation of symbols in a data stream, leading to intersymbol interference (ISI). Thus, it can limit the communication rate through the atmosphere, unless the effect is negligibly small or compensation techniques are used. Refractive index dispersion is intricately related to attenuation, as index of refraction and attenuation are related mathematically via the Kramers-Kronig relationship of the dielectric constant. Therefore, refractive index dispersion in the atmosphere depends on contributions from local absorption lines, dry air non-resonant spectrum, water vapor continuum spectrum, suspended water-droplets and rain [9]. For reasons of brevity we do not consider the effect in detail in this paper, but we note that GVD is relevant chiefly in wideband systems in frequency regions with a large group delay dispersion parameter. The effect on THz-pulses was investigated by Yang et al. [11]. The frequency can in principle be chosen such that GVD is small under reference conditions.

#### 3.2.2. Clear Air Turbulence

Clear air turbulence (CAT), and corresponding refractive index fluctuations, leads to effects directly perceivable at visible wavelengths and has a substantial impact on free-space optical (FSO) communication in the infrared. Atmospheric turbulence causes phase distortions; scintillation and beam wander, therefore causing intensity and phase fluctuations at the receiver and signal fading. While CAT is of limited relevance for frequencies below 10 GHz, it may become relevant for millimeter wave communication over large distances. In Figure 5, the probability density function for receiver irradiance after 300 km propagation through an isotropic atmosphere is shown based on the Rytov-method. At 1-THz transmission frequency, the probability density is spread out over a range of approximately 3 dB (an atmospheric structure constant, describing the strength of turbulence, of  $C_n^2 = 10^{-17} \text{ m}^{-2/3}$  is assumed). Therefore, CAT may have a noticeable effect on future millimeter-wave transmission systems, especially in air-to-ground communication; however of far less severity as compared

to laser-based systems.

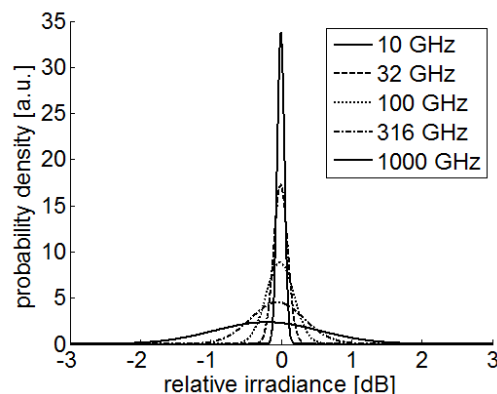


**Figure 5: Probability density functions of irradiance fluctuations in moderate strength clear air turbulence over 300 km distance (isotropic atmosphere assumed).**

Power fluctuations at the receiver must be considered in specifying the system design power margin in order to minimize the bit error rate (BER). The BER is determined by the overlapping region of the noise- and interference-broadened probability densities of power collected at the receiver, corresponding to different (e.g., “0” and “1”) states of the communication system. Within the overlapping region, the two states interfere and cannot be distinguished, thereby leading to bit errors with a certain probability. As power fluctuations due to turbulence are slow, compared to noise within the signal bandwidth, the received signal power can be tracked to dynamically set the decision threshold to maximize throughput and minimize BER for any signal level. Due to the large variability in received power levels (up to and beyond 40 dB dynamic range in optical systems [4]) agile power-adaptive techniques are required for the dynamic environment of air-to-air and -ground channels. However, signal fading may be inevitable and must be dealt with.

### 3.3. Refraction and Reflection

Due to the refractive index gradient in the atmosphere, radio beams are bent, typically towards the surface of the earth at higher frequencies, because of decreasing air density with altitude. This effect is beneficial to the transmission range of long-distance systems, due to the tendency of the beam to follow the curvature of the earth. However, we neglect the effect in the following.

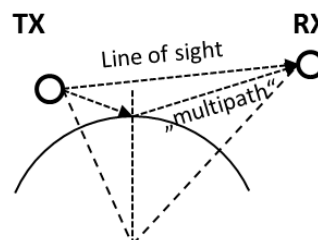


**Figure 6: Geometry to determine the specular multipath component in air-to-air communication.**

In terrestrial cellular communication, the vicinity of man-made and natural structures that absorb, refract and reflect



radio-waves leads to multi-path interference effects. In aeronautical communication, the separation from the ground typically renders these types of “scatterers” negligible. However, two principal effects relevant to high-flying aircraft are mentioned: reflections from the ground (non-line-of-sight) and reflections from aircraft components in the antenna vicinity. Both types of reflections are minimized by using highly directive antennas. Also, the reflectivity of rough surfaces depends on the ratio of surface roughness according to the Rayleigh-criterion, and higher frequencies tend to be dissipated by scattering, whereas low frequencies tend to be reflected according to the law of Snell [12]. However, over the ocean for example, strong and fluctuating reflectivity may be expected from the water surface even at high frequencies.

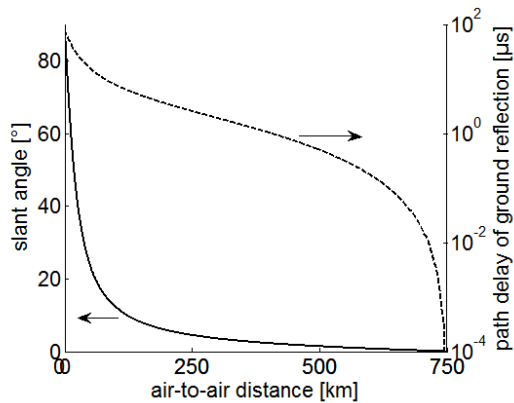


**Figure 7: Path delay of specular reflected component in an air-to-air transmission scenario (aircraft altitude: 11 km). The corresponding slant angle [°] is also shown.**

In order to determine the dominant, reflected component for an air-to-air link, the geometry shown in Figure 6 was used. Ground reflections lead to signal components with path delay that depends on aircraft separation and altitude in air-to-air communication. The path delay in microseconds is plotted in Figure 7 as function of aircraft separation in an air-to-air transmission scenario. The corresponding slant angle is also shown (the path delay follows the slant angle for distance  $\gg$  altitude, which is not apparent due to the log scale of path delay). Path delay is most severe at shorter distances, approaching ten microseconds for a line-of-sight path of 100 km, due to the large slant angles to the ground. At short distances, however, specular reflections are of less concern if directive antennas are used. The amplitude of the interfering signal depends on the elevation angle dependent antenna gain characteristics, and the amplitude and phase of the reflected wave depends on the angle of incidence. Assuming a 10-GHz wave reflecting from a flat air-seawater [13] boundary gives the complex reflectivity [14] as function of distance in the air-to-air scenario (Figure 8). The magnitude of the interfering signal at the receiver may thus be evaluated as function of transmitter and receiver antenna gain and reflectivity, both as function of reflection angle. For example, at 200-km distance the slant angle is  $6^\circ$ , and path delay

equals  $3.5 \mu\text{s}$ ; reflectivity is approximately 58%. The phase must also be taken into account, as especially the TE-wave phase is changed by  $180^\circ$  relative to the TM wave upon reflection. Fortunately, a 20-cm dish would theoretically offer sufficient directivity at 10 GHz to avoid the reflection at this distance (not considering side lobes in the beam pattern). Moreover, the reflected signal would be attenuated more strongly than the line-of-sight signal due to atmospheric layering.

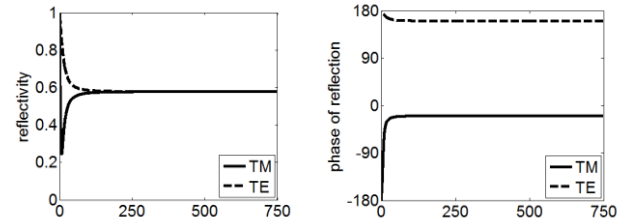


**Figure 8: Amplitude (left) and phase (right) of reflected wave as function of air-to-air distance (TM/TE: transversal magnetic/electric wave).**

Path delay due to multipath effects needs to be considered in wideband transmission channels, as the overlapping of signals leads to inter-symbol interference (ISI). In a first estimation, in the case of  $3.5\text{-}\mu\text{s}$  path delay spread the transmission rate of the communication channel should be below 45 kHz in a simple communication system [12]. In reality, if the signal-to-interference ratio (SIR) is low and signal processing techniques are used, much higher bandwidths can be achieved, however.

Moreover, specular reflection, as well as scattering, naturally may also occur due to weather phenomena (e.g., hydrometeors, turbulence). When multipath components are present in the signal with a delay spread surpassing the symbol rate, multi-antenna systems (Single/Multiple Input, Single/Multiple Output) may show potential also for aeronautical applications (e.g., [15]), due to the ability to separate one or several overlapping signals at the same carrier frequency, thereby increasing the overall transmission capacity by exploiting diversity gain.

## 4. TRANSMISSION SYSTEM

### 4.1. Technology Potentials: Power Transmission Efficiency

In telecommunication, frequency selection and antenna properties determine how much relative power can be transferred from transmitter to receiver, therefore determining the maximum theoretical channel capacity as function of receiver sensitivity (and channel characteristics). The received power in vacuum  $P_{RX}$  is given by Friis' transmission equation:

$$P_{RX} = G_{TX}G_{RX}P_{TX} \left( \frac{\lambda}{4\pi R} \right)^2$$

with transmit power  $P_{TX}$ , transmitter and receiver antenna gains  $G_{TX/RX}$ , wavelength  $\lambda = c/f$  ( $c$  = speed of light) and transmitter-receiver distance  $R$ , with the so-called “free-space loss factor” in parenthesis squared. The

formula suggests that attenuation increases with frequency; however, the loss factor is rather an antenna feature, as opposed to a propagation effect. For long-range communication, especially high-gain, or more precisely highly directive antennas are useful due to their ability to channel electromagnetic power into a defined solid angle, therefore delivering the signal to the intended receiver more efficiently. The gain (in the far field) of a parabolic antenna, for example, is defined as

$$G = \left(\frac{\pi d f}{c}\right)^2 e$$

with antenna diameter  $d$  (circular antenna), and an aperture and electric efficiency factor  $e$ . This indicates that, in a high-gain transmission system, the received power increases with  $f^2$  for a given antenna diameter, and with the aperture areas of transmitter and receiver ( $\sim d^4$ ). In Figure 9, the theoretical power transmission potential in vacuum is shown for transmission between two similar directive antennas<sup>11</sup> as function of  $\pi d^2 f/4$ .

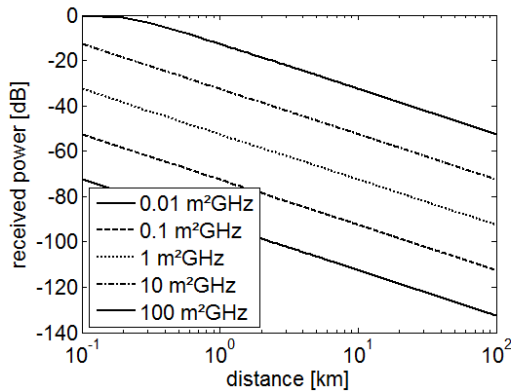


**Figure 9: Theoretically achievable power transmission between high-gain antennas, with antenna area x frequency as a parameter. A hypothetical 10-GHz system with 0.01 m² antenna area experiences -113 dB power loss over a 100-km path distance, for example.**

The figure illustrates that, in principle, by increasing the antenna frequency by a factor of 10, 20 dB can be gained in transmission efficiency. Consequently, relatively high frequency, directive antennas are typically used in high capacity satellite communications to cope with the large transmission distances, for example. Flat and shape-conformable, agile phased-array antennas [16] are therefore a technology option with considerable potential for aeronautical networking applications.

#### 4.2. Doppler Effect

Due to the velocity of high-flying commercial aircraft, the Doppler-effect is relevant to aeronautical transmission systems. A maximum velocity of M0.9 is assumed, corresponding to airspeed of 573 knots at altitude. The maximum (relative) Doppler-shift for electromagnetic

waves between two aircraft is thus approximately

$$\frac{\Delta f}{f_0} = \sqrt{\frac{c+v}{c-v}} - 1 = 3.5 \times 10^{-6}.$$

At 1 GHz carrier frequency, this amounts to a 3.5-kHz shift. In the infrared (carrier frequency: approx. 200 THz), the frequency would shift by 700 MHz, which is far beyond the linewidth of typical telecommunication lasers but much less compared to the dense-WDM grid spacing in fiber-optic systems<sup>12</sup>. Doppler is especially relevant for narrowband systems and modulation techniques, such as OFDM (orthogonal frequency division multiplexing) [14]. Therefore, special regard must be taken to frequency dependence in designing high-capacity aeronautical communication systems.

#### 4.3. Link Budget for Airborne Communication Networks

In the envisioned broadband communication scenario [2], broadband and directed air-to-air communication links are especially relevant. Most radio-propagation modeling considers slant-paths from ground to air or space, whereas (especially high bandwidth) air-to-air communication links are less explored due to the limited relevance in most (aeronautical or space) radio-communication scenarios. An air-to-air communication channel differs from an air-to-ground communication channel, mainly due to the structure of the atmosphere and the relevance of the path-integrated atmospheric influence.

We first define a model network based on a number of simple considerations to illustrate the feasibility of airborne networking. We assume that an airborne network is formed between 200 randomly distributed aircraft in a 5000x500x2 km³, ribbon-like corridor Figure 10. The number of aircraft is conservative with regard to peak air traffic count figures of the North Atlantic corridor [17]; however we do not consider factors affecting the spatial distribution (e.g., separation minima) of aircraft in this simple analysis.

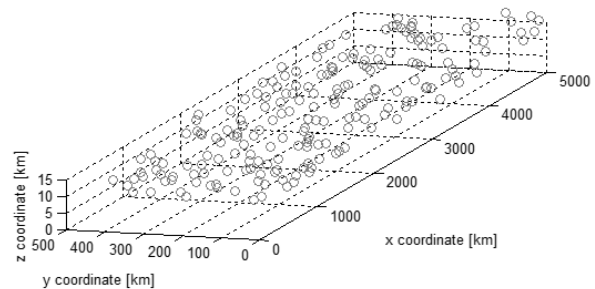


**Figure 10: Random aircraft distribution for a simple airborne network model.**

From the random aircraft distribution, the number of adjacent network nodes was computed for each simulated aircraft as function of air-to-air communication distance.

<sup>11</sup> The paraxial, Gaussian beam model was used, which is strictly valid for Gaussian beams with  $d > \frac{0.764 \text{ m}}{f[\text{GHz}]}$  [19].

<sup>12</sup> ITU-T G.694.1, "Spectral grids for WDM applications: DWDM frequency grid" (02/2012)

The result is shown in Figure 11, averaged for all aircraft.

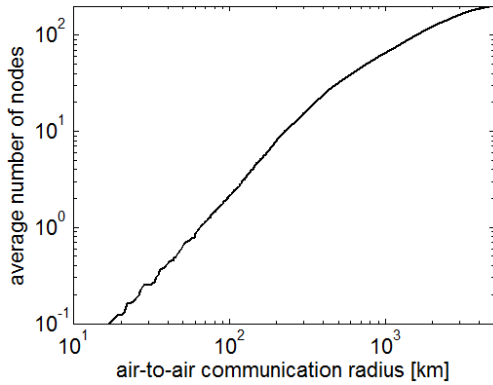


**Figure 11: Average number of aircraft (network nodes) as function of communication range.**

Below 500 km distance, within the width of the “ribbon”, there is a regime in which the aircraft number increases with the square of the distance. Beyond 500 km, the dependency tapers off to a linear dependence. Within a range of 100 km, on average two other aircraft are found. Within a range of 200 km, this number increases to 7.5, resembling the number of possible ad-hoc networking partners to form an airborne communication network. Within a 500 km radius, on average, more than 30 networking partners are available under the assumptions.

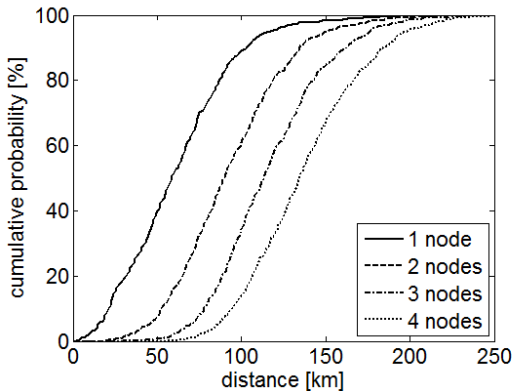


**Figure 12: Cumulative probability of finding a neighboring node, depending on communication radius.**

Moreover, the cumulative probability of finding a neighboring network node can be derived as function of communication range (Figure 12). At 200 km range, another network node can be found in our simulation with essentially 100% probability. At 250 km, the probability of finding 4 other network nodes approaches 100%. Therefore, a communication range of 250 km seems to be a reasonable requirement for communication equipment to enable sufficiently agile networking (the maximum geometric telecommunication distance for line-of-sight links is 750 km for aircraft flying at 11 km altitude, not considering refractive bending).

Next, we define three simple weather scenarios (ground temperature of 15°C, standard pressure of 1013 hPa at sea level assumed) for air-to-air link budget calculations:

**Table 2: Definition of weather scenarios.**

Scenario	Humidity at ground	Clouds + extent	Rain rate + extent
Dry	5 %	None	None
Humid	80 %	None	None
High-altitude cirrus	50 %	8/8 Cirrus (10-11.5 km)	None
Thunder-storm	100 %	8/8 Cumulo-nimbus (0.5-10 km)	10 mm/h (0-6 km)

These scenarios are evaluated, based on the atmospheric modeling and power budget considerations outlined above, assuming the following system specifications:

**Table 3: Definition of transmission systems.**

Frequency / wavelength	Antenna diameter [cm]	Bandwidth [GHz] (fractional)
5.6 GHz (e.g., WLAN)	20	0.04 (0.7%)
30 GHz (e.g., SatCom)	20	1 (3.3 %)
210 GHz (mmW)	20	5 (2.4 %)
1.67 μm (IR)	5	40 (0.02%)

For the dry scenario, the height-dependent attenuation curves shown in Figure 13, left are generated by the code (for the laser link, tabular values from [18] were interpolated – humidity dependence is not currently implemented in our laser transmission model). From the attenuation, the received power is calculated as a path function for each aircraft separation (Figure 13, right).

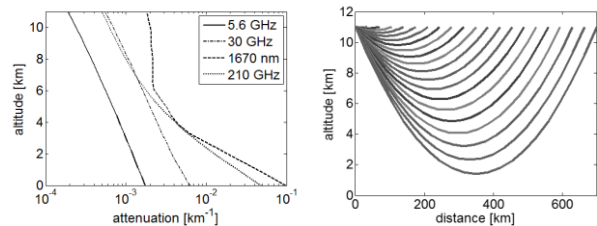


**Figure 13: (left) "Dry"-scenario attenuation as function of altitude; (right) air-to-air propagation paths as function of aircraft distance, relative to ground.**



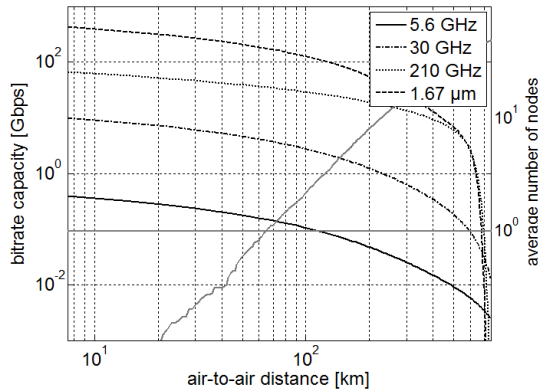


**Figure 14: Capacity-distance plot, assuming power-limited Shannon capacity (AWGN). Average number of nodes is superposed (gray line, cf. Figure 11).**

Next, we can estimate the Shannon bitrate capacity potential (Figure 14) based on the expected signal-to-noise ratio, assuming an antenna noise temperature and thermal background radiation (vacuum conditions assumed) in the case of radio frequency transmission, and assuming a noise-equivalent power of 250 nW in the case of the infrared system. An initial power level of 100 mW (20 dBm) was selected. As expected, the laser communication link has the highest potential in a clear and dry atmosphere, under the assumptions made (temporal effects are not considered in the Shannon

capacity estimation). The average number of airborne network nodes as function of distance is shown as well.

Now we compare the power transmission as function of aircraft separation for the defined weather scenarios, as an indication of the capacity potentials (Figure 15). In the “humid”-scenario, the maximum transmission distance is limited by high humidity and water vapor absorption in the troposphere. Stratospheric communication is not affected significantly due to the atmospheric layering, so essentially no effect is noticed at aircraft separation below 400 km. In the “cirrus”-scenario, laser communication is severely affected with around 5-dB attenuation assumed in the cloud. Transmission at 210 GHz recovers due to the fact that the beam travels below the cloud layer in our geometric assumption for some time at larger distances (the “jaggedness” of the curve is a numerical artefact from path discretization). The 5.6-GHz- and even 30-GHz-links are hardly affected. Lastly, in the “thunderstorm”-scenario, only the 5.6-GHz-link is able to penetrate the clouds with tolerable losses for some distance. All other frequencies are severely affected after short travel distances through the dense cloud.

In order to evaluate the usefulness of higher frequencies for aeronautical broadband communication, the transmission scenarios must be evaluated further. For example, in sufficiently dense airborne networks, local weather phenomena may be effectively circumvented by

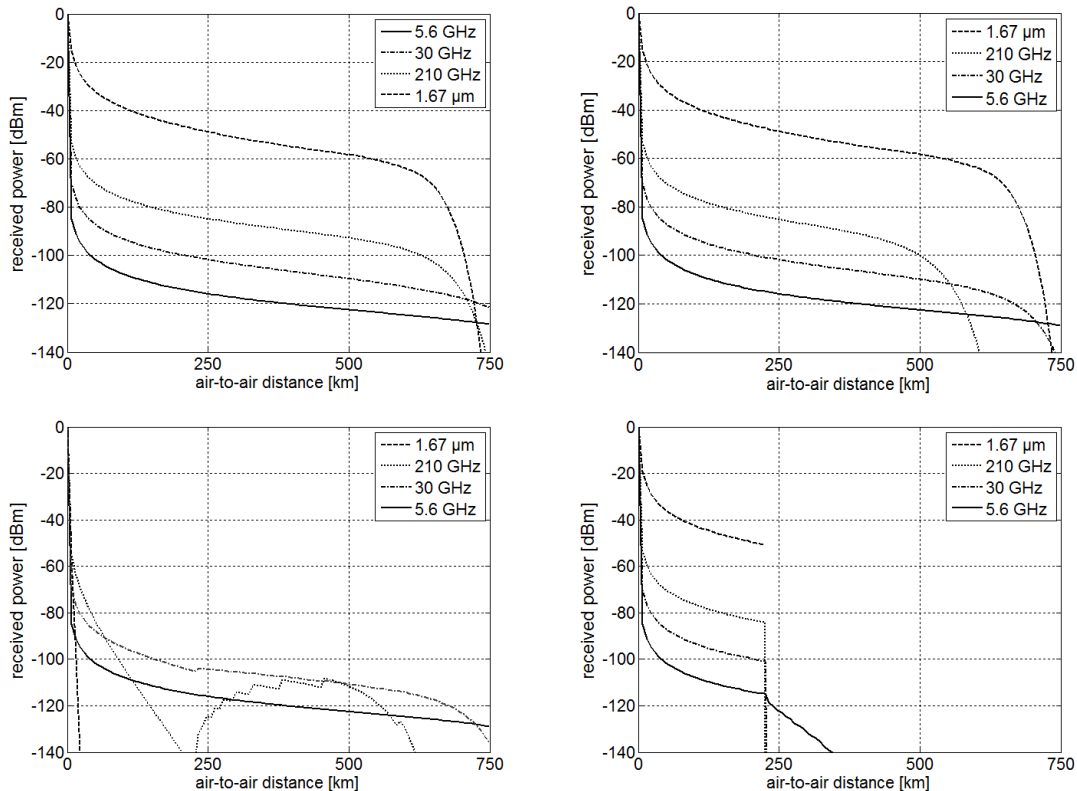


**Figure 15: Power transmission for the 4 weather scenarios (from top left to bottom right: dry, humid, cirrus, thunderstorm) as function of air-to-air distance. In the "cirrus"-scenario, laser transmission fails completely. In the "thunderstorm"-scenario, only 5.6-GHz transmission shows limited potential to penetrate clouds.**

ad-hoc network re-routing. We substantiate this claim by the fact that, in our simple network model, about ten aircraft can, on average, be found within a communication radius of 250 km. This is roughly the distance that can be covered in the case when high-altitude clouds, reaching up to 10 km altitude, block longer-distance transmission in our model. At high GHz-frequencies, thin cloud layer attenuation may be tolerated to a degree.

## 5. CONCLUSIONS

In this paper, atmospheric transmission impairments were discussed as a step to develop a framework in which technology options for high-bandwidth aeronautical telecommunication can be evaluated, based on fundamental considerations. A first evaluation of transmission at a number of frequencies in the GHz-range was performed for a number of weather scenarios. The performance was presented with regard to a benchmark laser communication system as a first step to evaluate high-bandwidth RF-photonics hybridization options for weather mitigation and ground access in airborne communication networks.

While only low GHz-frequency transmission offers weather resilience in all scenarios, more exotic transmission windows in the sub-THz frequency range may offer interesting high-bandwidth opportunities for air-to-air and air-to-satellite communication. In this regime, much bandwidth is available with limited interference potentials and therefore, possibly relaxed frequency allocation issues.

- [1] K.-D. Bächter, A. Reinhold, G. Stenz and A. Sizmann, "Drivers and Elements of Future Airborne Communication Networks," in *Deutscher Luft- und Raumfahrtkongress*, Berlin, Germany, 2012.
- [2] K.-D. Bächter, N. Randt and A. Sizmann, "Capacity Scaling in Airborne Communication Networks based on Air Traffic Scenario Modeling," in *Deutscher Luft- und Raumfahrtkongress*, Stuttgart, 2013.
- [3] H. Huang and et al., "100 Tbit/s free-space data link enabled by three-dimensional multiplexing of orbital angular momentum, polarization, and wavelength," *Optics Letters*, vol. 39, no. 2, pp. 197-200, 2014.
- [4] L. B. Stotts, L. C. Andrews, P. C. Cherry, J. J. Foshee, P. J. Kolodzy, W. K. McIntire, M. Northcott, R. L. Phillips, H. A. Pike, B. Stadler and D. W. Young, "Hybrid Optical RF Airborne Communications," *Proc. of the IEEE*, vol. 97, no. 6, pp. 1109-1127, 2009.
- [5] H. J. Liebe, "MPM - An Atmospheric Millimeter-wave Propagation Model," *Journal of Infrared and Millimeter Waves*, vol. 10, no. 6, pp. 631-650, 1989.
- [6] C. C. Chen, "Attenuation of electromagnetic radiation by haze, fog, clouds, and rain," *Rand Corp. Santa Monica, CA*, vol. 1694, no. PR, 1975.
- [7] L. S. Rothman and et al., "The HITRAN 2008 molecular spectroscopic database," *Journal of Quantitative Spectroscopic and Radiative Transfer*, vol. 110, no. 9, pp. 533-572, 2008.
- [8] N. Jacquinet-Husson, N. A. Scott, A. Chédin and A. A. Chursin, "The GEISA spectroscopic database system revisited for IASI direct radiative transfer modelling," *Atmos. Oceanic Opt.*, vol. 16, no. 3, pp. 256-261, 2003.
- [9] A. C. Valdez, Analysis of Atmospheric Effects due to Atmospheric Oxygen on a Wideband Digital Signal in the 60 GHz Band, Blacksburg, VA: M.Sc. Thesis, Virginia Polytechnic Institute and State University, 2001.
- [10] National Aeronautics and Space Administration (NASA), "U.S. Standard Atmosphere," U.S. Government Printing Office, Washington, D.C., 1976.
- [11] Y. Yang, M. Mandehgar and D. R. Grischkowsky, "Broadband THz Pulse Transmission Through the Atmosphere," *IEEE Trans. on Terahertz Science and Technology*, vol. 1, no. 1, pp. 264-272, September 2011.
- [12] A. Aragón-Zavala, J. Cuevas-Ruiz and J. Delgado-Penín, High-Altitude Platforms for Wireless Communications, Chichester, UK: John Wiley & Sons, Ltd., 2008.
- [13] R. Somaraju and J. Trunpf, "Frequency, temperature and salinity variation of the permittivity of Seawater," *IEEE Transactions on Antennas and Propagation*, vol. 54, no. 11, pp. 3441-3448, 2006.
- [14] A. F. Molisch, Wireless Communications Second Edition, Chichester, UK: Chichester, West Sussex, UK, 2011.
- [15] M. Rice and M. Jenson, "Multipath Propagation for Helicopter-to-Ground MIMO links," in *Military Communications Conference, MILCOM 2011*, Baltimore, MD, USA, 2011.
- [16] H. Schippers, P. Verpoorte, P. Jorna, A. Hulzinga, A. Meijerink, C. Roeloffzen, L. Zhuang, A. I. Marpaung, W. van Etten, R. G. Heideman, A. Leinse, A. Borreman, M. Hoekman and M. Wintels, "Broadband Conformal Phased Array with Optical Beam Forming for Airborne Satellite Communication," in *Aerospace Conference, Big Sky, MT*, 2008.
- [17] A. Pirovano, F. Garcia and J. Radzik, "Capacity Dimensioning for Aeronautical Communications in North Atlantic Corridor," in *19th Ka and Broadband Communications, Navigation and Earth Observation Conference*, Florence, Italy, 2013.
- [18] L. Elterman, "UV, Visible, and IR Attenuation for Altitudes to 50 km, 1968," *Environmental Research Papers*, no. 285, 1968.
- [19] A. E. Siegman, Lasers, University Science Books, 1986.